Larhyss Journal, ISSN 1112-3680, n°62, June 2025, pp. 7-35

IN-DEPTH INVESTIGATION OF FLOW MEASUREMENT USING SHARP-EDGED WIDTH CONSTRICTION IN TRAPEZOIDAL OPEN CHANNELS

ACHOUR B.[1*], AMARA L.[2], KULKARNI K.H.[3]

[1] Professor, Research Laboratory in Subterranean and Surface Hydraulics (LARHYSS), University of Biskra, PO Box 145, RP, Biskra, Algeria
[2] Associate Professor, Department of Civil Engineering and Hydraulics, Faculty of Science and Technology, University of Jijel, Algeria
[3] Associate Professor, Department of Civil Engineering, Dr Vishwanath Karad MIT World Peace University, 411038, Pune, India

(*) bachir.achour@larhyss.net

Research Article – Available at http://larhyss.net/ojs/index.php/larhyss/index
Received November 2, 2024, Received in revised form June 1, 2025, Accepted June 3, 2025

ABSTRACT

Flow measurement in open channels is a critical aspect of hydraulic engineering, essential for effective water resource management, irrigation, environmental monitoring, and industrial applications. The present study investigates the feasibility of using a sharp-edged width constriction as a reliable and efficient flow measurement device in trapezoidal open channels. The proposed device, which has already demonstrated its effectiveness in rectangular channels, consists of two thin vertical plates forming a full central rectangular opening, creating a lateral flow contraction. Its geometric simplicity, cost-effectiveness, and ease of implementation make it a promising alternative to conventional flow measurement structures.

The primary objective of this study is to establish a rigorous theoretical framework governing the discharge coefficient (C_d) of the device and validate it experimentally. The discharge coefficient, a crucial parameter in flow measurement, accounts for contraction effects, energy losses, and variations in velocity distribution. A comprehensive theoretical analysis is conducted using two independent methodologies. The first method is based on the energy equation, reformulated in dimensionless terms to explicitly incorporate the influence of approach flow velocity—an essential factor in accurate flow estimation. The second method employs the kinetic factor, which characterizes the relative approach velocity head. Both analytical approaches converge to the same result, demonstrating that the discharge coefficient (C_d) is governed exclusively by the compound dimensionless parameter ψ (β, M_1), which is intrinsically linked to the section reduction ratio. The parameter β, referred to as the contraction rate, is defined as $\beta = b_o/b$, where b_o denotes the opening width of the device, and b represents the base width of the trapezoidal approach channel. The dimensionless parameter M_1 is expressed as $M_1 = mh_1/b$, incorporating the influence of the trapezoidal approach channel's side slope (m), i.e., 1 vertical to m horizontal, and the relative upstream flow depth (h_1/b), both of which play a crucial role in determining the flow behavior and discharge characteristics. The contraction rate β provides critical insight into how geometric changes affect hydraulic behavior, and overall flow dynamics in open-channel systems. The exclusive dependence of C_d on β and M_1 is further confirmed through dimensional analysis.

The theoretical predictions are subjected to rigorous experimental validation. A large-scale experimental campaign was conducted under controlled laboratory conditions using a custom-built test setup equipped with precise measuring instruments. Seven different devices with varying contraction rates $0.15 \leq \beta \leq 0.45$ were tested, and an extensive dataset of 1,012 measurement points was collected. The experimental discharge coefficient values ($C_{d,Exp}$) were compared with theoretical predictions ($C_{d,Th}$), revealing a remarkable agreement, with a maximum deviation of only 0.301%. This minimal discrepancy underscores the reliability and the robustness of the derived (C_d) theoretical relationship and confirms that the device can be applied confidently in real-world hydraulic applications. This outstanding outcome enables practitioners to accurately estimate the desired flow rates conveyed through a trapezoidal channel with a high degree of confidence, eliminating the need for additional calibration efforts.

The findings of this study contribute significantly to the field of open channels flow measurement by providing a simple yet highly accurate alternative to conventional devices. The proposed device's self-cleaning ability, ease of installation, and precise theoretical predictability make it particularly suitable for applications in water distribution networks, drainage systems, irrigation canals, and environmental monitoring such as helping estimate river discharges, or providing accurate real-time hydrological data that supports decision-making in flood management

Keywords: Stage discharge relationship, Discharge, Flow measurement, Sharp-edged width constriction, Trapezoidal channel, Discharge coefficient.

INTRODUCTION

Flow measurement techniques must exhibit both high precision and reliability, ensuring consistency across various hydrological and industrial applications. These methods are indispensable in a wide range of fields, including industrial effluent monitoring, municipal water management, agricultural irrigation systems, and other critical hydraulic operations.

Accurate flow measurement serves multiple objectives, which must be clearly defined in advance to align with specific operational and environmental requirements. One of its key roles is in environmental monitoring, where it facilitates the assessment of pollutant loads in wastewater discharges, ensuring regulatory compliance and mitigating environmental impact. Additionally, flow measurement is essential for tracking variations in effluent discharge over time, providing critical data for process optimization and pollution control.

In hydraulic engineering, flow measurement plays a fundamental role in the design and optimization of hydraulic infrastructure, including pipelines, canals, treatment plants, and distribution networks. By precisely quantifying flow rates, engineers can ensure that systems are properly dimensioned and function efficiently, preventing issues such as overflows, pressure losses, or insufficient capacity.

Moreover, in the management of water resources, flow measurement is a key decision-making tool. It enables the quantification of available water reserves, essential for sustainable water allocation and conservation strategies. This is particularly crucial in groundwater resource management, where measuring the flow rates of wells, springs, and other water sources allows for the sustainable extraction and distribution of water to meet agricultural, industrial, and domestic demands.

More broadly, flow measurement plays a crucial role in quantifying water withdrawals, consumption, and discharge as part of in-situ monitoring programs. It enables municipalities, industries, and regulatory bodies to accurately assess the volumes of water extracted, utilized, or released within an urban area or economic installation, ensuring sustainable water management (Bahir et al., 2015).

Furthermore, flow measurement serves as a verification tool, allowing for the on-site validation of existing measurement systems using recognized verification methods (SIA, 1953; Achour et al., 2023; Qureshi et al., 2024). This ensures that installed flow meters and monitoring instruments provide accurate and reliable data, which is essential for effective decision-making, regulatory compliance, and resource optimization (Boutebba et al., 2014).

The primary objective of these approaches is to establish comprehensive assessments of water use and availability, thereby strengthening the regulatory framework. By holding water sector stakeholders accountable, these measures encourage the adoption of sustainable water management strategies (Faye, 2016; Jayasena et al., 2021), promoting responsible consumption, equitable distribution (Berrezel et al., 2023), and efficient resource allocation (Kouloughli and Telli, 2023; Kezzar and Souar, 2024).

A thorough understanding and application of flow measurement principles are fundamental for the proper implementation of an in-situ measurement system. Ensuring that these systems are accurately designed, calibrated, and maintained is critical to supporting data-driven decision-making in hydraulic engineering, environmental monitoring, and urban water management (Pandey et al., 2022; Aroua, 2023).

In practical applications, a wide range of users rely on flow measurement devices across multiple sectors, including municipal, industrial, and agricultural operations. These devices are essential for ensuring the precise monitoring and management of water resources, making them indispensable tools for utility managers, regulatory agencies, and environmental consultants.

In addition, consulting firms and auditing bodies employ flow measurement systems to verify the accuracy and reliability of installed instrumentation, ensuring compliance with industry standards and regulatory requirements. Water inspectors, hydraulic engineers, and technical professionals are particularly concerned with flow measurement, as it plays a crucial role in the design, optimization, and maintenance of water distribution systems (Rouissat and Smail, 2022), wastewater treatment facilities (Gaaloul, 2015; Aroua-Berkat and Aroua, 2022; Zaid and al., 2023), and irrigation networks (Rezzoug et al., 2016; Jelisavka and Goran, 2018; Derdour et al., 2022).

Given the diverse range of applications and stakeholders involved, the significance of flow measurement becomes evident. Its role extends beyond mere quantification of water flow; it serves as a cornerstone of sustainable water management (Bouly et al., 2019), infrastructure development, and environmental protection.

The flow under consideration pertains to free surface flow in open channels, a hydrodynamic regime characterized by a continuous interface between the flowing water and the atmosphere. Unlike pressurized conduit flows, free surface flow is governed by gravity-driven motion and is significantly influenced by factors such as channel geometry, slope, roughness, and external atmospheric conditions.

One of the most efficient and practical methods for determining flow rates in free surface flow conditions is the use of primary flow measurement devices, such as weirs. These devices, which are available in various geometric configurations, have undergone substantial theoretical and experimental advancements in recent years, enhancing their accuracy and applicability in hydraulic engineering. These weirs serve as fundamental tools in flow measurement, enabling engineers and researchers to assess discharge, monitor water distribution systems, and optimize hydraulic structures with greater efficiency (Remini, 2020).

Among the most widely used types are thin-crested weirs, which provide precise discharge measurements due to their well-defined flow characteristics, new triangular profile weir, called the 2A weir, designed to improve hydraulic performance and optimize flow regulation in open channels, broad-crested weirs, which offer greater flow stability and are particularly suitable for applications involving high flow rates and sediment transport considerations, and sharp-edged width constriction whose performance, simplicity and easy implementation have been proven (Achour and Amara, 2021a; 2021b; 2021c; 2021d; 2021e; Kulkarni and Hinge, 2021; Achour and Amara, 2022a; 2022b; 2022c; Achour and Amara, 2023a; 2023b; Kulkarni and Hinge, 2023).

It is highly relevant to emphasize that thin-crested and broad-crested sills serve purposes beyond flow measurement in open channels. These structures are also fundamental hydraulic components in the formation and the control of hydraulic jumps, which are essential for energy dissipation and flow stabilization (Achour et al., 2022e; Achour and Amara, 2023c). The formation and the control of the hydraulic jump significantly contribute to the protection of stilling basins, mitigating the erosive impact of tractive forces induced by high-velocity flows at work. This function is critical in preserving the structural integrity of hydraulic installations such as dams, preventing scour, and ensuring the long-term stability.

Furthermore, thin-crested and broad-crested sills play a pivotal economic role by enhancing the compactness and efficiency of stilling basins (Achour et al., 2022f). Their strategic integration within these hydraulic structures facilitates optimal energy dissipation, allowing for a more compact design without compromising hydraulic performance. This not only reduces construction costs and material requirements but also enhances the overall efficiency and longevity of stilling basins, making them more cost-effective and sustainable in hydraulic engineering applications.

Among the widely recognized methods for flow measurement in open channels, flumes stand out due to their well-established stage-discharge relationships and predefined discharge tables, which facilitate accurate flow quantification (Open Channel Flow, 2024). These hydraulic structures are extensively used in water resource management, irrigation systems, and environmental monitoring due to their reliability and ease of implementation. One of the oldest and most historically significant flow measurement flumes is the Parshall flume, which exemplifies the dynamic relationship between flow velocity and water depth variations (Parshall, 1936; Achour et al., 2003; Open Channel Flow, 2024). Similar to other critical flow measurement flumes with the same functionality (Bos, 1976; Hager, 1986; Achour et al., 2003; Open Channel Flow, 2024), the Parshall flume is engineered to induce a controlled acceleration of the flow through a gradual lateral contraction of its walls. As water enters the converging section of the Parshall flume, it accelerates progressively, reaching its maximum velocity at the control section within the narrow throat. The floor of this throat is deliberately sloped downward, causing a substantial drop in the water level. This hydraulic behavior ensures the formation of a critical flow condition, which serves as the basis for flow rate determination in open channel environments. Due to its proven acceptable accuracy, minimal head loss, and adaptability, the Parshall flume remains a preferred choice for hydraulic engineers, water managers, and environmental scientists involved in flow monitoring and water distribution optimization.

The scientific literature also highlights a variety of innovative flow measurement devices, each distinguished by its unique design, operational efficiency, and applicability. These devices have been developed to enhance measurement accuracy, optimize hydraulic performance, and adapt to diverse hydrological conditions. Their original configurations and engineering advancements make them valuable alternatives for various flow monitoring, water management applications, and even flood management (Hountondji et al., 2019; Bekhira et al., 2019). These include Replogle-Bos-Clemens (RBC) flumes (Replogle, 1975), cutthroat flumes proposed by Skogerboe et al. (1972), the Montana flume, in both its original and modified forms (Westesen, 1992; Open Channel Flow, 2024; Achour et al., 2025), SM-Flume (Samani and Magallanez, 2000), and circular flumes (Samani et al., 1991), and the list is not exhaustive.

Through the application of dimensional analysis, Ferro (2016) developed a theoretical stage-discharge relationship for the central baffle flume, providing a fundamental framework for flow measurement in open channels. This theoretical model was subsequently calibrated and refined using the experimental findings of Peruginelli and Bonacci (1997), ensuring greater accuracy and practical applicability. Further advancements in the study of central baffle flumes were made through experimental investigations conducted by Kolavani et al. (2019), Bijankhan and Ferro (2019), and Aniruddha et al. (2020). These studies systematically examined the influence of various geometric parameters on the hydraulic performance and flow behavior within the flume. Their findings contributed to a deeper understanding of flow dynamics, energy dissipation, and discharge characteristics, paving the way for enhanced design optimization and improved measurement accuracy in hydraulic engineering applications.

It is worth highlighting that recent advancements in flume design have led to the development and testing of new and more efficient flow measurement flumes. These innovatively engineered flumes exhibit exceptional accuracy and reliability in their stage-discharge relationships, surpassing traditional designs in precision and performance. Moreover, their remarkably simple installation process, and their property of being of a universal range, enhances their practical applicability across a wide range of hydraulic and environmental monitoring systems (Achour and De Lapray, 2023; Achour et al., 2024).

This study explores the feasibility of utilizing a sharp-edged width constriction as an innovative flow measurement solution in trapezoidal open channels. This investigation builds upon the successful implementation and validation of the same device by Achour and Amara (2021f; 2022d), where it was rigorously tested and proven to be a highly effective and precise flow measurement system in a rectangular approach channel. By extending its application to trapezoidal channels, this research aims to evaluate its hydraulic performance, adaptability, and measurement accuracy within a broader range of hydraulic conditions. This device represents the simplest and most streamlined flow measurement system conceived, consisting solely of two thin vertical plates installed perpendicular to the flow direction. These plates are strategically positioned to create a full rectangular central opening of width bo, through which the water passes. The opening width bo is always less than or equal to the base width b of the trapezoidal approach channel, thereby establishing a contraction rate defined as $\beta = bo/b$, which remains less than or equal to unity in all scenarios. When $\beta = 1$, the flow experiences minimal contraction, preserving the natural flow profile with only a slight reduction in cross-sectional area.

The benefits of the proposed device significantly outweigh its limitations, rendering it a highly viable and efficient solution for practical flow measurement applications. One of its most notable advantages lies in its exceptionally simple design, comprising only two thin vertical plates. This minimalist configuration not only facilitates straightforward fabrication and installation but also eliminates the structural complexities and implementation challenges commonly encountered with other flow measurement systems of comparable functionality. Its ease of deployment makes it an ideal choice for a wide range of hydraulic applications, ensuring both cost-effectiveness and operational efficiency.

The proposed device is designed for seamless installation and removal, requiring minimal effort for both deployment and maintenance. A key feature of its structural design is that the bottom of the approach channel, where the thin plates are positioned, remains perfectly level, free from local elevations or sills. This ensures that the longitudinal axis of the channel remains entirely horizontal, preserving the natural flow dynamics. As a direct consequence of this optimized configuration, the device possesses an intrinsic self-cleaning capability, allowing it to automatically clear any small debris transported by the water flow, thereby minimizing blockages and maintenance requirements.

The other significant advantage of the advocated device lies in its theoretical controllability, enabling the precise analytical prediction of both its discharge coefficient and the corresponding flow rate. This capability, which will be rigorously demonstrated in this study, ensures high measurement accuracy and reliability, distinguishing the device from conventional flow measurement systems.

Despite its numerous advantages, the device presents only a few limitations. The most notable and potentially restrictive drawback is its rectangular notch cross-section, which delivers optimal measurement accuracy primarily for larger upstream flow depths. To mitigate this issue, the authors strongly recommend adopting a contraction rate β within the experimentally validated range of $0.15 \leq \beta \leq 0.45$. The selection of this specific range was neither arbitrary nor coincidental; rather, it was based on proven and reliable previous hydraulic considerations (Achour and Amara, 2022d) to ensure that the upstream flow depth remains sufficiently large, thereby promoting a stable, undisturbed free surface that facilitates precise gauge readings.

Furthermore, to ensure the highest level of measurement precision**,** the authors strongly recommend the use of a double-precision Vernier gauge**,** an advanced instrument allowing reading flow depths with an exceptional absolute precision of ±0.02 mm, as documented by Achour and Amara (2022d)**.** The integration of this high-precision measuring tool significantly enhances the reliability, consistency, and repeatability of flow measurements obtained with the proposed device, ensuring superior accuracy in hydraulic assessments and operational efficiency in practical applications.

The primary objective of this study is to establish theoretical relationships governing the discharge coefficient (C_d) of the proposed device through an approach that is both rigorously formulated and scientifically compelling. The intended theoretical framework must explicitly incorporate the influence of the approach flow velocity, a crucial parameter in the field of flow measurement, as its effect cannot be overlooked in achieving accurate discharge predictions. Prior to engaging in this theoretical derivation, a dimensional analysis will serve as a fundamental preliminary step, facilitating the identification of key influential parameters that must be considered to develop a comprehensive and robust governing equation for the device.

The final phase of this study will focus on the experimental validation of the proposed theoretical relationships or, if necessary, their refinement through a corrective factor derived from a comprehensive analysis of observational data.

To achieve this objective, an extensive experimental campaign will be conducted using a custom-designed hydraulic testing facility, specifically engineered to ensure optimal measurement accuracy. This installation will be equipped with high-precision instrumentation, allowing for the rigorous assessment of the device under realistic hydraulic conditions. A series of tests will be meticulously performed on multiple configurations, incorporating various opening widths (b_o) to examine their impact on flow behavior and discharge characteristics.

The authors aim to systematically collect a representative dataset of measurement points, ensuring that the resulting analysis yields robust, reliable, and scientifically meaningful conclusions. This empirical validation process will serve to confirm the accuracy of the theoretical models while providing a solid foundation for further refinement, if required.

MATERIAL AND METHODS

Description of the device and the resulting flow

Fig. 1 presents a perspective view of the sharp-edged width constriction under consideration, featuring an opening width b_o, positioned perpendicularly to the flow direction within a trapezoidal approach channel with a base width b.

The vertical plates forming the sharp-edged constriction are expected to play the role of a Q-flow rate measurement. It is the simplest flow measurement structure ever devised.

The thin vertical plates are securely anchored to the lateral sides and base of the approach channel, embedded within the thickness of the channel walls and bottom. A precisely engineered indentation is incorporated along the inner perimeter of the concerned cross-section to accommodate this configuration (Fig. 2). The plates can be reinforced with structural elements on their downstream face to enhance their resistance against hydrostatic pressure forces, particularly at greater upstream flow depths h_1 (Achour and Amara, 2022d).

Fig. 3 presents an upstream-facing front view, illustrating both the approach channel and the sharp-edged width constriction. Meanwhile, Figs. 4a and 4b depict the plan view of the sharp-edged width constriction embedded within the trapezoidal channel and the longitudinal profile of the resulting flow, respectively.

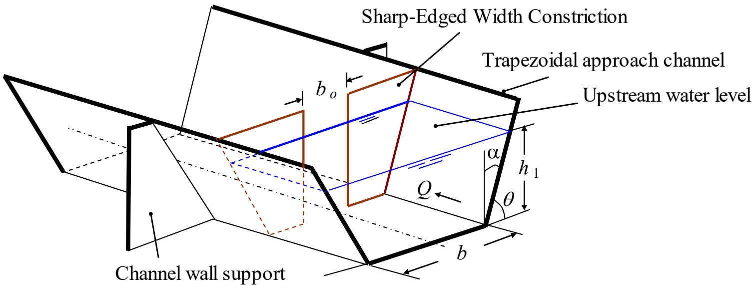

Figure 1: Definition sketch of a sharp-edged constriction in a trapezoidal open channel

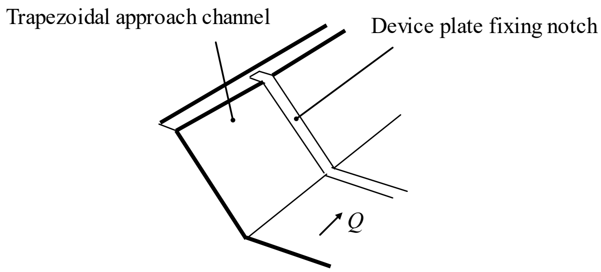

Figure 2: Detail of the notch for fixing the vertical plates of the device

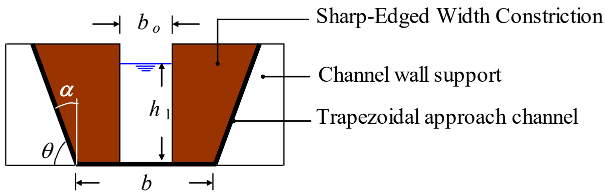

Figure 3: Front view from upstream

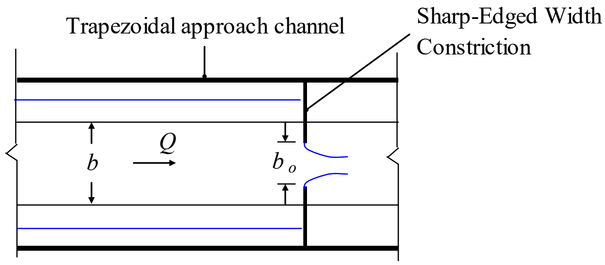

a)

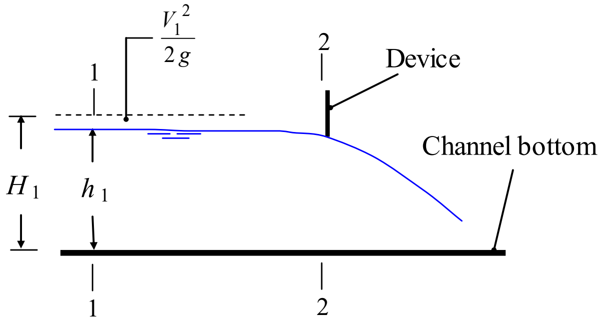

b)

Figure 4: a) Plan view of the trapezoidal approach channel and device and b) the resulting flow longitudinal profile

Owing to its geometric simplicity, the proposed structure is highly cost-effective compared to most conventional flow measurement devices, as it consists solely of two thin plates with a thickness ranging between 1.5 mm and 2 mm. As a result, it is by far the least expensive and most cost-effective flow measurement device.

Furthermore, this compact device is highly space-efficient, as it belongs to the category of short open-channel flow measurement structures, extending vertically rather than longitudinally.

Additionally, the device exhibits remarkable versatility, as it can be utilized in open channels of various geometries across multiple industrial sectors. Its applications extend to effluent flow measurement in treatment plants, diversion channels designed to manage peak stream flows, municipal sewage systems, and irrigation canals. Furthermore, owing to its minimalistic design, consisting of only two thin plates, the device is both simple to construct and easy to implement.

The plates can be fabricated from aluminum when lightweight properties and abrasion resistance are prioritized. Alternatively, they can be constructed from stainless steel, as employed in the present experimental study, to ensure enhanced durability and structural integrity.

Furthermore, as the plates are designed such that the approach channel bottom remains level, with neither a step rise nor a drop (Figs. 1 and 4), debris transported by the flow does not accumulate upstream of the plates. Instead, it is swiftly carried away by the current, endowing the device with an intrinsic self-cleaning capability.

The installation of thin vertical plates positioned perpendicularly to the flow direction results in an increase in upstream water levels, as illustrated in Fig. 4b. The smaller the opening width b_o, the greater the rise in upstream water level. Under these conditions, the upstream flow remains in a subcritical state, ensuring a smooth, undisturbed free surface, leading to a highly precise gauge reading of the flow depth. This upstream flow condition was consistently observed by the authors throughout the experimental tests.

Conversely, as the opening width b_o increases, free surface disturbances become more pronounced, leading to reduced precision in gauge readings of the upstream flow depth h_1. Furthermore, the accuracy of h_1 measurements improves as h_1 increases. To ensure optimal measurement conditions, a threshold value for the contraction rate $\beta = b_o/b$ should preferably not be exceeded.

The authors' observations have demonstrated that the optimal range for the contraction rate β lies between 0.15 and 0.45 ($0.15 \leq \beta \leq 0.45$). This is the same range previously examined by the authors in their study of the notch under consideration, when implemented within a rectangular approach channel (Achour and Amara, 2021f; 2022d).

The configuration illustrated in Fig. 4a operates on the principle of lateral flow contraction, inducing critical flow conditions at section 2-2 (Fig. 4b). Even with the plates' thickness reduced to just a few millimeters, a well-defined control section naturally forms at section 2-2. The flow regime remains subcritical between sections 1-1 and 2-2, transitions to critical at section 2-2, and becomes supercritical downstream of this section. This transition results in a sudden drop in the liquid mass as it exits the narrow opening b_o. The formation of a control section is an indispensable prerequisite for the proper operation of the device as an effective flow measurement instrument in open channels. Furthermore, as will be demonstrated later, the prevailing critical flow condition at section 2-2 plays a crucial role in establishing the theoretical discharge coefficient relationship.

As shown in Fig. 1, the initial wetted area A_1 before reduction can be expressed as follows:

$$A_1 = b h_1 + m h_1^2 \tag{1}$$

where m is the side slope of the trapezoidal approach channel, i.e., 1 vertical to m horizontal, (Fig. 3) expressed as follows:

$$m = \mathrm{cotg}(\theta) = \mathrm{tg}(\alpha) \tag{2}$$

The initial water cross-sectional area A_1 is constricted to the water cross-sectional area A_o within the slit, as expressed below:

$$A_o = b_o h_1 \tag{3}$$

Let us define the section reduction ratio (ζ) as the ratio of A_1 to A_o such that:

$$\zeta = \frac{b_o h_1}{b h_1 + m h_1^2} \tag{4}$$

Eq. (4) can be written in dimensionless terms as follows:

$$\zeta = \frac{\beta}{1+M_1} \tag{5}$$

where

$$M_1 = \frac{m\,h_1}{b} \tag{6}$$

The dimensionless parameter ζ can be regarded as a dimensionless compound parameter, as it exclusively depends on both the contraction rate β and the dimensionless parameter M_1, which incorporates the effects of the trapezoidal approach channel's side slope m and the relative upstream flow depth h_1/b. This interdependence reflects the combined influence of geometric contraction and flow conditions on the discharge coefficient. Indeed, it will be shown that the section reduction ratio (ζ) is the sole influencing factor upon which the device's discharge coefficient C_d exclusively depends.

On the other hand, it is important to recall that β represents the contraction rate, defined as $\beta = b_0/b$.

Dimensional analysis and discharge coefficient dependency

This section is expected to express the discharge coefficient C_d sought in literal form, i.e., using symbols representing the physical quantities on which C_d depends. This helps to understand the functional dependence of C_d on the parameters and variables on which it depends. Each physical quantity will be treated as a function, not a number or a set of numbers. The dimensional analysis proves to be very powerful for obtaining the functional relationship of the discharge coefficient C_d provided all the influential parameters are listed. This is the first step required by dimensional analysis, which often calls on intuition. The functional relationship relating the influential parameters to each other will be transformed into a completely different relationship grouping dimensionless variables. As a result, the number of influential parameters is reduced, and dimensionless quantities play an important role in any physical phenomenon because the governing laws generally depend on relative values rather than absolute values.

However, it must be remembered that dimensional analysis is only an intuitive and approximate method that does not guarantee the integrity of the reasoning, and the final result or the relationship governing the discharge coefficient is not possibly true only up to a constant. In other words, only rigorous reasoning-based theory will lead to more accurate results. This is what this study intends to do with the greatest rigor.

Intuitively, the key parameters influencing the current phenomenon can be identified as follows: the discharge Q passing through the rectangular notch of the device, the upstream flow depth h_1 (Fig. 1), the base width b of the trapezoidal approach channel, the constriction opening width b_o, the inclination angle θ of the approach channel side wall (Fig. 3), the acceleration due to gravity g, the density ρ of the flowing water, the surface tension σ, and the dynamic viscosity μ of the fluid. Thus, a total of nine influential parameters have been identified, which can be interrelated through the following functional expression:

$$f\left(Q, h_1, \theta, b, b_o, \rho, \mu, \sigma, g\right) = 0 \tag{7}$$

Applying the Vashy-Buckingham π theorem (Langhaar, 1962) and recognizing that the angle θ is related to m as expressed in Eq. (2), leads to the derivation of the following flow rate relationship, which governs the device exclusively in terms of dimensionless parameters:

$$Q = g^{1/2} b_o\, h_1^{3/2} \varphi\left(\frac{\rho g h_1^{3/2}}{\mu}, \frac{\rho g h_1^2}{\sigma}, \frac{b_o}{b}, \frac{m h_1}{b}\right) \tag{8}$$

In addition, Eq. (8) can be reformulated into the following well-established stage-discharge relationship:

$$Q = C_d\, g^{1/2} b_o\, h_1^{3/2} \tag{9}$$

Thus, it can be observed that the symbol φ represents the functional dependence of the discharge coefficient C_d.

However, in the case of a rectangular cross-section, such as the opening of the device under consideration, the discharge Q is more conventionally expressed in the following form:

$$Q = \frac{2}{3} C_d \sqrt{2g}\, b_o\, h_1^{3/2} \tag{10}$$

On the other hand, in Eq. (8), the first two dimensionless parameters in the functional relationship φ can be readily identified as the Reynolds number Re and the Weber number We, respectively. Furthermore, the final two parameters correspond to the contraction rate β and M_1, as defined in Eq. (6). Consequently, the C_d governing functional relationship can be expressed as follows:

$$C_d = \varphi\left(Re, We, \beta, M_1\right) \tag{11}$$

In the context of the present study, the flow regime is turbulent, characterized by high Reynolds numbers (Re), indicating that viscous effects are negligible. In addition, surface tension effects are typically noticeable only at low flow rates or when the central openings of the device are extremely narrow. However, this is not applicable to the current research, as the test installation is large, and the range of flow rates examined is broad and representative of practical conditions. Consequently, the Weber number (We) has a negligible influence on both the flow rate and the flow behavior.

In considering the previous inferences, Eq. (11) simplifies to the following:

$$C_d = \varphi\left(\beta, M_1\right) \tag{12}$$

Thus, Eq. (12) demonstrates that the discharge coefficient C_d of the device is influenced by both the contraction rate β and the dimensionless parameter M_1. This implies that C_d is directly affected by the device's contraction ratio, the trapezoidal approach channel side slope m, i.e., 1 vertical to m horizontal, and the relative upstream flow depth h_1/b. However, these theoretical inferences must be substantiated through both rigorous analytical validation and empirical analysis, which will be systematically addressed in the following sections.

It is important to recall that both β and M_1 are the sole parameters affecting the section reduction ratio ζ as defined by Eq. (5).

Theoretical discharge coefficient relationship

Energy-based derivation of the discharge coefficient

This section is dedicated to deriving the theoretical relationship governing the discharge coefficient C_d of the device when implemented in a trapezoidal open channel. The theoretical approach adopted will be both rigorous and precise, meticulously considering the influence of the approach flow velocity. This effect is explicitly represented by the velocity head $V_1^2/(2g)$, as illustrated in Fig. 4b, where V_1 denotes the mean approach flow velocity.

The critical depth in the rectangular notch of Fig. 3 can be expressed as follows:

$$h_c = \left(\frac{Q^2}{g\,b_o^2}\right)^{1/3} \tag{13}$$

When considering Eq. (1), the total head H_1 in section 1-1 (Fig. 4b) can be expressed as follows:

$$H_1 = h_1 + \frac{Q^2}{2g\left(b\,h_1 + m\,h_1^2\right)^2} \tag{14}$$

Taking into account Eqs. (6) and (13), Eq. (14) can be rewritten as follows after some rearrangement:

$$H_1 = h_1 + \frac{\beta^2\,h_c^3}{2\,h_1^2\left(1+M_1\right)^2} \tag{15}$$

Let us define the following dimensionless parameters:

$$h_1^* = \frac{h_1}{h_c} \tag{16}$$

$$H_1^* = \frac{H_1}{h_c} \tag{17}$$

Note that since $h_1 > h_c$, then $h_1^* > 1$.

In addition, dividing the two sides of Eq. (15) by h_c and taking into account Eqs. (16) and (17) results in the following:

$$H_1^* = h_1^* + \frac{\beta^2}{2\,h_1^{*2}\left(1+M_1\right)^2} \tag{18}$$

Furthermore, since critical flow prevails in section 2-2 at the location of the rectangular notch (Fig. 4b), one may write the following:

$$H_{2,c} = \frac{3}{2}h_c \tag{19}$$

That is,

$$H_{2,c}^* = \frac{3}{2} \tag{20}$$

where

$$H_{2,c}^* = \frac{H_{2,c}}{h_c} \tag{21}$$

Over the short distance between sections 1-1 and 2-2 (Fig. 4b), head losses can be considered negligible, as their influence on the final result is insignificant. Consequently, one may write $H_1^* = H_{2,c}^* = 3/2$. Eq. (18) then reduces to the following:

$$h_1^* + \frac{\beta^2}{2\,h_1^{*2}\left(1+M_1\right)^2} = \frac{3}{2} \tag{22}$$

Eq. (22) is a cubic equation in h_1^* that can be written in the following form:

$$h_1^{*3} - \frac{3}{2}h_1^{*2} + \frac{\beta^2}{2\left(1+M_1\right)^2} = 0 \tag{23}$$

Note that the last term of Eq. (23) corresponds to half the square of the section reduction ratio ζ expressed by Eq. (5), i.e., $\zeta^2 / 2$.

To simplify the writing, let us define ψ as follows:

$$\psi = \frac{\beta^2}{2\left(1+M_1\right)^2} \tag{24}$$

Thus, Eq. (23) reduces to the following:

$$h_1^{*3} - \frac{3}{2} h_1^{*2} + \psi = 0 \tag{25}$$

By applying the cubic equation resolution method proposed by Spiegel (1974), it can be demonstrated that the discriminant of Eq. (25) is negative, signifying the existence of three real roots. Among these, the following solution is the only one that satisfies the condition h1* > 1 and must therefore be retained:

$$h_1^* = \frac{1}{2} + \cos\left[\frac{1}{3}\cos^{-1}\left(1-4\psi\right)\right] \tag{26}$$

When considering Eq. (13), the discharge Q through the rectangular notch can be written as follows:

$$Q = \sqrt{g}\, b_o\, h_c^{3/2} \tag{13a}$$

Eliminating h_c between Eqs. (16) and (13a) yields the following:

$$Q = \sqrt{g}\, b_o \frac{h_1^{3/2}}{h_1^{*\,3/2}} \tag{27}$$

Eq. (27) can be rewritten under the following form:

$$Q = \frac{2}{3}\left(\frac{3}{2}\right)\frac{1}{\sqrt{2}}\sqrt{2g}\, b_o \frac{h_1^{3/2}}{h_1^{*\,3/2}} \tag{28}$$

A comparison of Eqs. (10) and (28) yields the following exact discharge coefficient relationship:

$$C_{d,Th} = \frac{3}{2\sqrt{2}} h_1^{*\,-3/2} \tag{29}$$

where the subscript "*Th*" denotes "Theoretical".

Substituting Eq. (26) into Eq. (29) and performing the necessary simplifications lead to the following final theoretical discharge coefficient expression:

$$C_{d,Th} = 3\left\{1+2\cos\left[\frac{1}{3}\cos^{-1}\left(1-4\psi\right)\right]\right\}^{-3/2} \tag{30}$$

Eq. (30) establishes the theoretical discharge coefficient governing the device under consideration. As rigorously demonstrated by this theoretical formulation, C_d depends exclusively on the dimensionless parameter $\psi(\beta;M_1)$, as anticipated through dimensional analysis.

It is noteworthy that as ψ approaches zero, which corresponds to large values of the relative upstream depth h_1/b ($M_1\rightarrow\infty$) according to Eqs. (6) and (24), the discharge coefficient C_d asymptotically converges to the constant value $1/\sqrt{3}$, according to Eq. (30). Conversely, when M_1 approaches zero ($M_1\rightarrow 0$), which corresponds to the side slope $m = 0$ as per Eq. (6), the configuration transitions to that of a rectangular approach channel. This specific case has been extensively studied by Achour and Amara (2021f; 2022d). For this configuration, the discharge coefficient C_d remains governed by Eq. (30), where $\psi = \beta^2/2$, and $\beta = b_o/b$ has been previously defined as the contraction rate, with, as a reminder, b representing the width of the rectangular approach channel. Thus, Eq. (30) applies to both trapezoidal and rectangular approach channels, demonstrating its general validity across different channel geometries.

Eq. (10), in conjunction with Eq. (30), enables the calculation of the sought discharge Q conveyed through the trapezoidal channel under consideration.

Kinetic factor approach for discharge coefficient derivation

The total head H_1 in section 1-1 of Fig. 4b can be written in the following form:

$$H_1 = \left(1+\delta\right)h_1 \tag{31}$$

where δ represents a kinetic factor, expressed as a specific fraction of h_1, and is also associated with the following relative approach velocity head $V_1^2/(2gh_1)$.

It can be readily demonstrated that Eq. (31) can be reformulated as follows:

$$H_1^* = \left(1+\delta\right)h_1^* \tag{32}$$

Rearranging Eq. (18) into the format of Eq. (32) yields the following governing relationship for δ:

$$\delta = \frac{\beta^2}{2\, h_1^{*\,3}\, \left(1 + M_1\right)^2} \tag{33}$$

Considering Eq. (24), Eq. (33) reduces to the following:

$$\delta = \frac{\psi}{h_1^{*\,3}} \tag{34}$$

It is important to emphasize that, in accordance with Eq. (26), h_1* is solely a function of the dimensionless parameter ψ. Consequently, it follows that the kinetic factor δ is entirely governed by ψ, as established in Eq. (34).

Furthermore, the flow rate Q passing through the rectangular notch is expressed by Eq. (13) as follows:

$$Q = \sqrt{g}\, b_o\, h_c^{3/2} \tag{13a}$$

The critical depth h_c is related to the total head H_1 as follows:

$$h_c = \frac{2}{3} H_1 \tag{35}$$

Inserting Eq. (31) into Eq. (35) yields the following:

$$h_c = \frac{2}{3} (1 + \delta)\, h_1 \tag{36}$$

Additionally, Eq. (13a) can be rewritten in the following form:

$$Q = \frac{1}{\sqrt{2}} \times \frac{2}{3} \times \frac{3}{2} \sqrt{2g}\, b_o \left(\frac{2}{3}\right)^{3/2} (1 + \delta)^{3/2}\, h_1^{3/2} \tag{37}$$

Comparing Eqs. (10) and (37) the following discharge coefficient relationship is derived:

$$C_d = \frac{1}{\sqrt{2}} \times \frac{3}{2} \times \left(\frac{2}{3}\right)^{3/2} (1 + \delta)^{3/2} \tag{38}$$

Following the necessary calculations, the final expression is obtained as follows:

$$C_d = \frac{1}{\sqrt{3}}\, (1 + \delta)^{3/2} \tag{39}$$

An analysis of Equation (39) reveals that if the approach flow velocity were to be neglected, implying $\delta \to 0$, the discharge coefficient of the device in question would be reduced to a constant value of $1/\sqrt{3}$. However, this assumption is inherently flawed, as it overlooks the critical influence of the approach flow velocity on the discharge coefficient, resulting in an inaccurate depiction of the flow behavior. This contradicts Cd's Eq. (12), which has been rigorously derived through dimensional analysis.

In the domain of flow measurement, disregarding the approach flow velocity can have severe consequences, potentially resulting in significant inaccuracies in the computation of the discharge coefficient Cd, and hence of the flow rate Q.

On the other hand, inserting Eq. (34) into Eq. (39) results in the following:

$$C_d = \frac{1}{\sqrt{3}}\left(1 + \frac{\psi}{h_1^{*3}}\right)^{3/2} \tag{40}$$

This represents the final discharge coefficient relationship, derived from the fundamental properties of the kinetic factor δ. Despite being established through two distinct methodologies, Eqs. (30) and (40) yield precisely the same result, demonstrating their theoretical consistency.

As established in the analysis of Eq. (30), Eq. (40) further corroborates that as ψ approaches zero, the discharge coefficient C_d converges to the constant value $1/\sqrt{3}$.

Laboratory validation of the theoretical discharge coefficient model

The primary objective of this section of the study is to validate or, if necessary, refine the theoretical discharge coefficient relationship given by Eq. (30) through experimental testing of multiple devices with varying opening widths.

The experimental setup depicted in Fig. 5 illustrates the installation used to evaluate the proposed device. The setup features an opening width b_0 positioned within a trapezoidal approach channel with a base width of 25 cm, a top width of 65.41 cm, and an inclination angle of 60° relative to the horizontal, corresponding to $m = 1/\sqrt{3}$. The approach channel had a depth of 35 cm.

The primary objective of the tests was to collect experimental data pairs (Q_{Exp}, $h_{1,Exp}$), for various configurations of the device, i.e., for different opening widths b_0. This data collection aimed to compute the experimental discharge coefficient $C_{d,Exp}$ and compare it to the theoretical discharge coefficient $C_{d,Th}$ as defined by Eq. (30). The experimental discharge coefficient was determined using Eq. (10), expressed as follows:

$$C_{d,Exp} = \frac{\frac{3}{2} Q_{Exp}}{\sqrt{2g}\, b_o\, h_{1,Exp}^{3/2}} \tag{41}$$

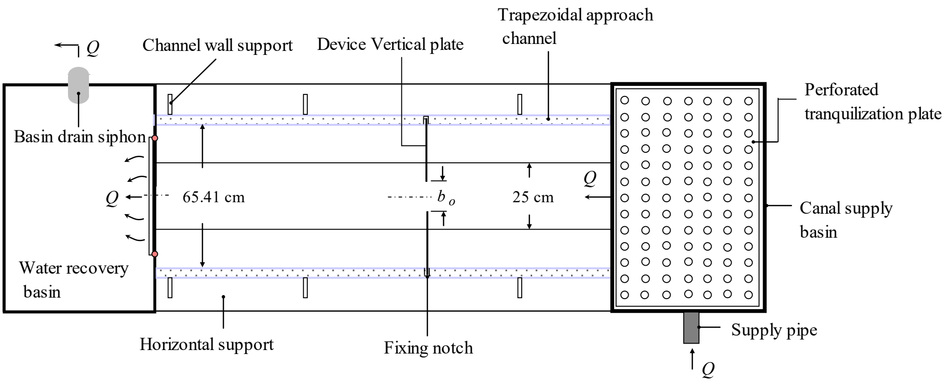

Figure 5: Experimental setup utilized for device testing

The flow rate Q_{Exp} was determined experimentally by averaging the measurements obtained from ultrasonic and electromagnetic flow meters. The upstream depth h_1 was precisely measured using a double-precision Vernier gauge, which was thoroughly described by the authors Achour and Amara (2022d) in a previous study. Consequently, the measurement instruments employed in the experiments ensured exceptional accuracy and reliability.

Seven experimental devices were designed and tested, covering contraction rates within the range $0.15 \le \beta \le 0.45$. The experimental setup, illustrated in Fig. 5, along with its accompanying equipment, facilitated the collection of 1,012 measurement points (Q-h_1 pairs). The flow rates and upstream flow depths were systematically varied within the ranges 0.23 l/s $\le Q_{Exp} \le$ 38.74 l/s and 2.35 cm $\le h_{1,Exp} \le$ 34.374 cm, respectively.

Table 1 provides a summary of the test conditions corresponding to each of the seven experimental devices.

Table 1: Experimental parameter ranges for each of the seven tested devices

Device	Number of measurements	b_o (cm)	Discharge range (Q, l/s)	Range of upstream depths (h_1, cm)	Range of M_1
1	188	3.75	[0.23; 13.10]	[2.35; 34.74]	[0.0543; 0.8023]
2	146	5.00	[0.37; 17.38]	[2.65; 34.55]	[0.0612; 0.7979]
3	133	6.25	[0.54; 21.80]	[2.92; 34.60]	[0.0674; 0.7990]
4	132	7.50	[0.69; 26.07]	[3.05; 34.49]	[0.0704; 0.7965]
5	149	8.75	[0.94; 30.43]	[3.35; 34.43]	[0.0774; 0.7951]
6	125	10.00	[1.19; 35.02]	[3.57; 34.57]	[0.0824; 0.7983]
7	139	11.25	[1.44; 38.74]	[3.74; 34.10]	[0.0864; 0.7875]

The experimental parameter values Q_{Exp} and $h_{1,\mathrm{Exp}}$ listed in columns 4 and 5 of Table 1, respectively, were used to compute the experimental discharge coefficients in accordance with Eq. (41). The resulting experimental discharge coefficients are depicted in Fig. 6 as discrete markers plotted against M_1 for each tested contraction rate β. Additionally, the solid lines in the same figure represent the theoretical discharge coefficients, computed using Eq. (30) in conjunction with Eq. (24).

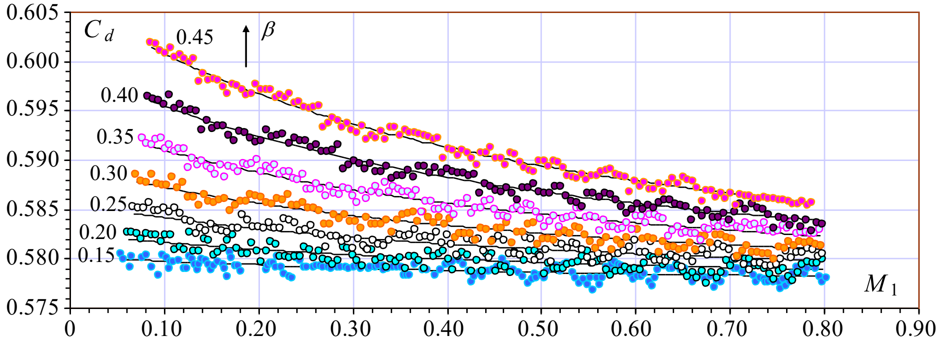

Figure 6: Variation of C_d as a function of M_1 for the tested contraction rates β. (—) Theoretical values derived from Eq. (30); The markers represent the authors' experimental observations.

Thus, as illustrated in Fig. 6, there is a strong correlation between the experimental and theoretical values of the discharge coefficient C_d. The experimental data points are well distributed around the theoretical curve, with deviations that remain within a satisfactory range, meeting the practitioner's expectations and achieving the desired performance levels. This observation is further corroborated by Table 2, which presents the distribution of deviations for each of the seven tested devices.

Moreover, as depicted in Fig. 6, when $M_1 \to \infty$, the curves asymptotically converge to a horizontal line, approaching a constant discharge coefficient previously determined as $C_{d,Th} = 1/\sqrt{3} = 0.57735027$.

Table 2: Deviation between theoretical and experimental discharge coefficient values for each of the seven tested devices

Device	Contraction rate β	Deviation $\Delta C_d / C_d$ (%)		
		Minimum	Maximum	Average
1	0.15	0.00144	0.301	0.0857
2	0.20	0.0082	0.301	0.1052
3	0.25	0.01075	0.215	0.1041
4	0.30	0.00895	0.213	0.0946
5	0.35	0.00111	0.218	0.0898
6	0.40	0.00711	0.210	0.0851
7	0.45	0.0072	0.212	0.0784

Table 2 reinforces the remarkable agreement between theoretical predictions and experimental results, as the maximum deviation between $C_{d,Th}$ and $C_{d,Exp}$ does not exceed 0.301%. Accordingly, Eq. (30), which governs the discharge coefficient of the proposed device, remains fully valid in its current form, requiring no modifications or corrections. As a result, users can confidently apply this equation with high precision to determine the discharge coefficient C_d and, consequently, the flow rate Q sought, as expressed in Eq. (10).

CONCLUSION

After successfully testing the device during a recent study as a means of flow-measuring in a rectangular approach channel, the present investigation extrapolated its use to the case of the trapezoidal channel, which is a common channel in practice. The device was formed of two thin plates arranged to achieve a central opening smaller than the channel base width, causing a lateral contraction of the inflow cross-section. This geometric configuration allowed defining the contraction rate $\beta = b_o/b$, which is less or equal to unity, where b is the base width of the trapezoidal approach channel and b_o is the width of the device's central opening.

The device is devoid of crest height, meaning that the flow crossing the central opening of the device does not undergo any vertical contraction, giving the device a self-cleaning character, meaning it easily passes sediments and smaller debris. Claiming to use this means to measure flow rates in open channels amounts to defining the theoretical relationship governing the discharge coefficient, then deducting that governing the flow rate. To predict this important coefficient, a theory was built under the credible hypothesis of the appearance of a control section in the narrowed section of the device. This is the prerequisite condition for the correct functioning of the device under consideration. One should know that the transition from a subcritical flow regime upstream of the device to a supercritical regime downstream is necessarily accompanied by a control section that the authors observed during testing. Therefore, the considered contraction can perfectly play the role of a flow-measuring tool. Another simplifying assumption, as important as the first, has been adopted considering no head loss between the device and the upstream depth measurement section. This hypothesis was acceptable since the distance separating the two involved sections was sufficiently short.

Thus, the study's objective was twofold; the first was to apply a rigorous and convincing theory capable of deducing the relationships governing the discharge coefficient (C_d) and the flow rate (Q), while accounting for the effect of the approach flow velocity. The second objective was to test several devices with different central openings, subjected to practical flow conditions. These tests aimed to confirm the reliability of the derived theoretical relationship governing the device's discharge coefficient C_d.

From the theoretical point of view, both the stage-discharge relationship and the discharge coefficient relationship sought were derived by applying two different methods, which nevertheless gave the same result. The first method was based on the transformed energy equation in dimensionless terms, and the second method was based on the properties of the kinetic factor closely related to the approach flow velocity. Both methods confirmed that the discharge coefficient (C_d) of the advocated device depends exclusively on the compound dimensionless parameter ψ, which is a function of the contraction rate β and the dimensionless parameter $M_1 = mh_1/b$, where m is the side slope of the trapezoidal approach channel walls, and h_1 is the upstream flow depth. Thus, β, m, and h_1/b are the influential parameters.

The validity and reliability of the theoretical discharge coefficient C_d relationship, and hence that of the flow rate (Q), has been confirmed by analyzing sample tests of more than a thousand measurement points of the pair (Q;h).

The analysis of the observations was able to conclude that the derived governing C_d theoretical relationship can be used with great confidence, without any correction, to estimate the flow rate (Q) conveyed by the trapezoidal channel, with 0.301% as a maximum deviation.

In the field of flow measurement, the authors recommend practitioners to select and adopt a device that permits analytical calculation and theoretical development as it is crucial for ensuring accuracy, predictability, and reliability. Devices designed with theoretical foundations enable the derivation of explicit equations governing flow behavior. Theoretical models allow for accurate predictions of flow rates across different conditions, making the measurement method adaptable to varying hydraulic environments. A well-defined mathematical formulation ensures that results are not solely dependent on empirical data, which may be limited in scope. A device that supports theoretical development reduces the reliance on extensive experimental calibration, which can be time-consuming and costly. It enables self-calibrating methods, where the discharge coefficient (C_d) or flow rate (Q) can be determined using analytical expressions rather than being estimated purely from empirical data. Theoretical models help identify and quantify systematic errors, ensuring higher precision in flow rate estimation. Devices with a strong theoretical basis can be scaled up or down to different flow conditions without requiring new experimental testing each time. The ability to generalize flow equations means the device can be applied in various hydraulic environments, e.g., irrigation channels, drainage systems, environmental monitoring. It allows engineers to optimize designs for different channel geometries, such as rectangular, trapezoidal, or natural streams while maintaining reliable performance. Relying solely on experimental data may lead to inaccuracies when applying the device to unseen conditions, referring to hydraulic or environmental scenarios that were not explicitly tested during experimental validation but may arise when the device is deployed in real-world applications. If a flow measurement device relies solely on experimental data without a strong theoretical foundation, its accuracy and reliability may be compromised when faced with these untested conditions.

In addition, a device supported by theoretical development minimizes the need for extensive field trials under every new configuration. In cases where experimental validation is required, a pre-established theoretical framework significantly simplifies the process by providing a baseline for comparison. Theoretical equations help identify critical flow transitions, such as the shift from subcritical to supercritical flow, ensuring the device remains accurate in all conditions. They provide insights into factors affecting discharge coefficients, energy losses, and contraction effects, which are essential for maintaining device efficiency in practical applications.

OVERVIEW OF THE KEY FINDINGS

The paper investigates a simple and innovative device for flow measurement in trapezoidal open channels using a sharp-edged width constriction with a rectangular opening. The study combines rigorous theoretical development with experimental validation to propose a cost-effective and highly accurate method for measuring flow rates in trapezoidal open channels.

Device Design and Concept

The proposed device consists of two thin vertical plates forming a central opening (b_0) that is narrower than the trapezoidal channel's base width (b). This design creates a contraction in the flow, effectively altering the hydraulic behavior to allow accurate flow measurement. The simplicity of the design allows easy implementation and self-cleaning properties due to the absence of any obstruction on the approach channel floor.

Theoretical Development

Two distinct methods, both of which had stringently given the same result, based on the energy equation and the kinetic factor related to the approach flow velocity, were used to derive the discharge coefficient (C_d) relationship. Both methods confirm that C_d depends exclusively on the parameter ψ, a dimensionless parameter which is a function of the contraction rate $\beta = b_0/b$ and $M_1 = mh_1/b$. This means that β, m, and h_1/b are the governing parameters influencing the discharge coefficient. This finding has been confirmed through dimensional analysis.

Experimental Validation

A total of 1,012 measurement points were collected from seven devices with varying contraction rates such as $0.15 \leq \beta \leq 0.45$. The experimental discharge coefficient $C_{d,Exp}$ closely matched the theoretical predictions $C_{d,Th}$ with a maximum deviation of only 0.301%. This excellent agreement demonstrates the reliability of the theoretical model and confirms that the device can be applied without the need for additional calibration.

Practical Implications

The device's accuracy, simplicity, and low cost make it ideal for applications in irrigation systems, drainage channels, sewage systems, and environmental monitoring. The recommended contraction rate $0.15 \leq \beta \leq 0.45$ ensures accurate flow measurement without surface disturbances.

The design's self-cleaning nature prevents debris accumulation, making it suitable for long-term operation in practical hydraulic environments.

Declaration of competing interest

The authors declare that they have no known competing financial interests or personal relationships that could have appeared to influence the work reported in this paper.

REFERENCES

ACHOUR B., BOUZIANE T., NEBBAR K. (2003). Triangular broad-crested weir in a rectangular channel, 1st Part, Larhyss Journal, No 2, pp. 7-43. (In French)

ACHOUR B., AMARA L. (2021a). Theoretical discharge coefficient relationship for contracted and suppressed rectangular weirs, Larhyss Journal, No 45, pp. 165-182.

ACHOUR B., AMARA L. (2021b). Discharge coefficient of a parabolic weir, theory and experimental analysis, Larhyss Journal, No 46, pp. 77-88.

ACHOUR B., AMARA L. (2021c). Theoretical discharge coefficient relationship for a contracted triangular notch weir, Experimental analysis for the special case of the 90-degree V-notch, Larhyss Journal, No 46, pp. 89-100.

ACHOUR B., AMARA L. (2021d). Discharge coefficient for a triangular notch weir, theory and experimental analysis, Larhyss Journal, No 46, pp. 7-19.

ACHOUR B., AMARA L. (2021f). Discharge measurement in a rectangular open-channel using a sharp-edged width constriction, theory and experimental validation, Larhyss Journal, No 45, pp. 141–163.

ACHOUR B., AMARA L. (2022a). Accurate discharge coefficient relationship for the Crump weir, Larhyss Journal, No 52, pp. 93-115.

ACHOUR B., AMARA L. (2022b). Triangular broad-crested Weir, Theory and Experiment, Larhyss Journal, No 49, pp. 37-66.

ACHOUR B., AMARA L. (2022c). Rectangular broad-crested flow meter with lateral contraction, Theory and Experiment, Larhyss Journal, No 49, pp. 85-112.

ACHOUR B., AMARA L. (2022d). Discharge coefficient relationship for the sharp-edged width constriction - new theory and experiment, Flow Measurement and Instrumentation, Vol. 88, Paper ID 102269, pp. 1-16.

ACHOUR B., AMARA L., MEHTA D. (2022e). Control of the hydraulic jump by a thin-crested sill in a rectangular channel - new experimental considerations, Larhyss Journal, No 50, pp. 31-48.

ACHOUR B., AMARA L., MEHTA D., BALAGANESAN P.4 (2022f). Compactness of hydraulic jump rectangular stilling basins using a Broad-crested sill, Larhyss Journal, No 51, pp. 31-41.

ACHOUR B., AMARA L. (2023a). The 2A triangular weir - design, theory, and experiment, Larhyss Journal, No 55, pp. 191-213.

ACHOUR B., AMARA L. (2023b). Discharge coefficient relationship for the SMBF flume, Larhyss Journal, No 53, pp. 95-115.

ACHOUR B., AMARA L. (2023c). Control of the hydraulic jump by a Broad-crested sill in a rectangular channel-new theory and experiment, Larhyss Journal, No 54, pp. 145-174.

ACHOUR B., De LAPRAY G. (2023). Curved wall triangular flume (CWTF), Design, Theory, and Experiment, Larhyss Journal, No 56, pp. 139-178.

ACHOUR B., MEHTA D., AZAMATHULLA H.M. (2024). A new trapezoidal flume for open channel flow measurement - Design, Theory, and Experiment, Larhyss Journal, No 59, pp. 157-179.

ACHOUR B., AMARA L., KULKARNI K.H. (2025). Development and validation of a modified H-flume for accurate flow measurement in rectangular channels, Larhyss Journal, No 61, pp. 241-286.

AMARA L., ACHOUR B. (2021e). Theoretical approach to stage-discharge relationship for a circular sharp-crested weir, Larhyss Journal, No 46, pp. 101-113.

ANIRUDDHA D.G., ANKUR K., AVINASH B.M. (2020). Cylindrical central baffle flume for flow measurements in open channels, Technical Note, Journal of Irrigation and Drainage Engineering, Vol. 146, Issue 9, pp. 1–9.

AROUA N. (2023). Setting out urban water issues examples from Algeria and worldwide, Larhyss Journal, No 56, pp. 309-327.

AROUA-BERKAT S., AROUA N. (2022). Opportunities and challenges for wastewater reuse in Algeria, Larhyss Journal, No 51, pp. 7-17.

BAHIR M., EL MOUKHAYAR R., CARREIRA P. SOUHEL A. (2015). Isotopic tools for groundwater management in semi-arid area: case of the wadi Ouazzi basin (Morocco), Larhyss Journal, No 23, pp. 23-39.

BEKHIRA A., HABI M., MORSLI B. (2019). The management of flood risk and development of watercourses in urban areas: case of the town of Bechar, Larhyss Journal, No 37, pp. 75-92. (In French)

BERREZEL Y.A. ABDELBAKI C., ROUISSAT B., BOUMAAZA T., KHALDOON A.M. (2023). Decision support system for the management of water distribution networks a case study of Tourville, Algeria, Larhyss Journal, No 54, pp. 7-24.

BIJANKHAN M., FERRO V. (2019). Experimental study on triangular central baffle flume, Flow Measurement and Instrumentation, Vol. 70, Paper ID 101641.

BOS M.G. (1976). Discharge measurement structures, hydraulic laboratory, Wageningen, The Netherlands, Report 4.

BOULY S., CISSE A., FAYE C. (2019). Problematic of storm water management in cities in developing countries: case of Santhiaba and Belfort district (commune of Ziguinchor, Senegal), Larhyss Journal, No 39, pp. 313-331.

BOUTEBBA K., BOUZIANE M.T., BOUAMRANE A. (2014). Decision-making aid for optimizing the management of drinking water supply networks, Larhyss Journal, No 20, pp. 279-296. (In French)

DERDOUR A., BELAM N., CHEBAB W. (2022). Traditional irrigation system and methods of water harvesting in the oasis of Sfissifa Ksour mountains – Algeria, Larhyss Journal, No 49, pp. 17-35.

FAYE C. (2016). Management of water resources in the local of Ndondol: study of community management of water resources and water use conflicts in Mbomboye villages (Senegal), Larhyss Journal, No 25, pp. 219-240. (In French)

FERRO V. (2016). Simple flume with a central baffle, Flow Measurement and Instrumentation, Vol.52, pp. 53–56.

GAALOUL N. (2015). Modeling of underground flows in unsaturated porous medium: application to artificial recharge by treated wastewater - Korba coastal water table (cap-bon, Tunisia), Larhyss Journal, No 21, pp. 181-190. (In French)

HAGER W.H. (1986). Discharge Measurement Structures, Communication 1, Department of Civil Engineering, Federal Polytechnic School of Lausanne, Switzerland. (In French)

HOUNTONDJI B., CODO F.P., DAHOUNTO S.V.H., GBAGUIDI T.B. (2019). Flood management in urban environment: case of the Cotonou city in Benin, Larhyss Journal, No 39, pp. 333-347. (In French)

JELISAVKA B., GORAN R. (2018). Irrigation of agricultural land in Montenegro: overview, Larhyss Journal, No 33, pp. 7-24.

JAYASENA H.A.H., RATHNAYAKE R.D.D.P., CHANDRASENA M.G.P.N., RANATHUNGA B.P.D.W. (2021). A classic example of urban-rural linkages through ancient Voda Ela in Sri Lanka - symbiosis of total environment on efficient water management, Larhyss Journal, No 47, pp. 59-82.

KEZZAR M., SOUAR A. (2024). The water management system in the village of Menades in Algeria between past and present, Larhyss Journal, No 57, pp. 55-79.

KOLAVANI F.L., BIJANKHAN M., STEFANO C., DI FERRO V., MAZDEH A.M. (2019). Experimental study of central baffle flume, Journal of Irrigation and Drainage Engineering, Vol. 145, Issue 3.

KOULOUGHLI C.E., TELLI A. (2023). Modern water supply management techniques and methods: a review, Larhyss Journal, No 55, pp. 7-23.

KULKARNI K.H., HINGE G.A. (2021). Performance enhancement in discharge measurement by compound broad crested weir with additive manufacturing, Larhyss Journal, No 48, pp. 169-188.

KULKARNI K.H., HINGE G.A. (2023). An energy perspective of composite broad crested weir for measuring accurate discharge, Larhyss Journal, No 54, pp. 85-106.

LANGHAAR H.L. (1962). Dimensional Analysis and Theory of Models, Wiley and Sons Inc.

OPEN CHANNEL FLOW. (2024). Brochures, Flow Tables, Instructions for Flumes, Manholes, Shelters, and Weirs, Atlanta, USA. Website accessible at https://www.openchannelflow.com/support/downloads-center

PANDEY P., MISHRA R., CHAUHAN R.K. (2022). Future prospects in the implementation of a real-time smart water supply management and water quality monitoring system, Larhyss Journal, No 51, pp. 237-252.

PARSHALL R.L. (1936). The improved Venturi flumes, Transaction, ASCE, Vol. 89, pp. 841–880.

PERUGINELLI A., BONACCI F. (1997). Mobile prisms for flow measurement in rectangular channels, Journal of Irrigation and Drainage Engineering, Vol. 123, Issue 3, pp. 170–174.

QURESHI H.U., ABBAS I., SHAH S.M.H., TEO F.Y. (2024). Hydrologic evaluation of monthly and annual groundwater recharge dynamics for a sustainable groundwater resources management in Quetta city, Pakistan, Larhyss Journal, No 60, pp. 27-53.

REMINI B. (2020). Oued M'Zab's I.R.S development population and floods, life in harmony Part 1: hydraulic structures, Larhyss Journal, No 42, pp. 63-95.

REPLOGLE J.A. (1975). Critical flow flumes with complex cross sections, in: Proceedings, Irrigation and Drainage Division, Specialty Conference, ASCE, New York, pp. 336–338.

REZZOUG C., REMINI B., HAMOUDI S. (2016). Modern irrigation in oasis of Lahmar (Bechar, Algeria): problems and consequences, Larhyss Journal, No 25, pp. 259-267. (In French)

ROUISSAT B., SMAIL N. (2022). Contribution of water resource systems analysis for the dynamics of territorial rebalancing, case of Tafna system, Algeria, Larhyss Journal, No 50, pp. 69-94.

SAMANI Z., JORAT S., YOUSEF M. (1991). Hydraulic characteristics of circular flume, Journal of Irrigation and Drainage Engineering, ASCE, Vol. 117, Issue 4, pp. 558–566.

SAMANI Z., MAGALLANEZ H. (2000). Simple flume for flow measurement in open channel, Journal of Irrigation and Drainage Engineering, ASCE, Vol. 126, Issue 2, pp. 127–129.

SIA (1953). Contribution to the study of gauging methods, Bulletin 18, Schweiz Bureau Wasserfoschung (Swiss Water Research Office), Bern, Switzerland. (In French)

SKOGERBOE G.V., BENNETT R.S., WALKER W.R. (1972). Generalized discharge relations for cutthroat flumes, Journal of Irrigation and Drainage Engineering, ASCE, Vol. 98, Issue 4, pp. 569–583.

SPIEGEL M.R. (1974). Mathematical Handbook of Formulas and Tables, Twentieth Edition, McGraw Hill Inc, New York, USA.

WESTESEN G.L. (1992). Montana (Short Parshall) Flume (Part 1), Water measurement, MT 9121 (AG).

ZAIDI K., DJEDDOU M., SEKIOU F., HAMEED I.A., SHAWAQFAH M. (2023). Predictive modelling of daily dried sludge production in full-scale wastewater treatment plant using different machine learning combined with empirical mode decomposition, Larhyss Journal, No 56, pp. 77-106.